ELECTRODIFFUSION OF IONS APPROACHING THE MOUTH OF A CONDUCTING MEMBRANE CHANNEL

ARTHUR PESKOFF* AND DONALD M. BERS[‡]
*Departments of Biomathematics and Physiology, University of California, Los Angeles, California
90024-1766; and ‡Division of Biomedical Sciences, University of California, Riverside, California
92521-0121

ABSTRACT   The movement of ions in the aqueous medium as they approach the mouth (radius a) of a conducting membrane channel is analyzed. Starting with the Nernst-Planck and Poisson equations, we derive a nonlinear integrodifferential equation for the electric potential, $\phi(r)$, $a \leq r < \infty$. The formulation allows deviations from charge neutrality and dependence of $\phi(r)$ on ion flux. A numerical solution is obtained by converting the equation to an integral equation that is solved by an iterative method for an assumed mouth potential, combined with a shooting method to adjust the mouth potential until the numerical solution agrees with an asymptotic expansion of the potential at $r - a \gg \lambda$ (λ = Debye length). Approximate analytic solutions are obtained by assuming charge neutrality (Läuger, 1976) and by linearizing. The linear approximation agrees with the exact solution under most physiological conditions, but the charge-neutrality solution is only valid for $r \gg \lambda$ and thus cannot be used unless $a \gg \lambda$. Families of curves of ion flux vs. potential drop across the electrolyte, $\phi(\infty) - \phi(a)$, and of permeant ion density at the channel mouth, $n_1(a)$, vs. flux are obtained for different values of a/λ and $S = a \, d\phi/dr(a)$. If $a \ll \lambda$ and $S = 0$, the maximum flux (which is approached when $n_1(a) \rightarrow 0$) is reduced by 50% compared to the value predicted by the charge-neutrality solution. Access resistance is shown to be a factor $a/[2(a + \lambda)]$ times the published formula (Hille, 1968), which was derived without including deviations from charge neutrality and ion density gradients and hence does not apply when there is no counter-ion current. The results are applied to an idealized diffusion-limited channel with symmetric electrolytes. For $S = 0$, the current/voltage curves saturate at a value dependent on a/λ; for $S > 0$ they increase linearly for large voltage.

INTRODUCTION

Measurements to determine the conductance of an ion channel are affected by the characteristics of the electrolytes in contact with the two ends of the channel. For sufficiently low ion density or high electric driving potential, the flux of ions through a channel can be influenced more by the electrodiffusion of ions through the electrolyte, in the region immediately external to the channel mouth, than by the intrinsic channel properties (Läuger, 1976; Andersen, 1983a and b). It is therefore important to understand the current-voltage-ion density relationships within an electrolyte. Up to this time, this problem has not been analyzed completely.

A great deal has been published on this subject for various special cases in which a force affecting the ion motion (such as density gradient or electric potential gradient) is not included, or some approximation (such as linearization or assumption of charge neutrality) is made. To understand the range of validity of these results, it is helpful to solve the complete problem and then consider the special cases as particular limits of the general solution.

The classical treatment of an electrolyte is the Debye-Hückel theory (1923), in which the radial distribution of electric potential and charge surrounding a spherically symmetric charge is obtained by solving the linearized Poisson-Boltzmann equation. The central charge is surrounded by a cloud of opposite charge which screens the central charge within several Debye lengths, λ. The nonlinear Poisson-Boltzmann equation with spherical symmetry was later solved numerically (Guggenheim, 1959). The one-dimensional nonlinear Poisson-Boltzmann equation for the electrolyte adjacent to a charged planar membrane was solved analytically (Gouy, 1910; Chapman, 1913). Numerical solutions have been obtained for more complicated geometries that include the electrolyte and channel vestibules (Dani, 1986). The Poisson-Boltzmann equation describes the limiting case, in which there is no ion flux, of the present problem.

With ion current flowing radially inward from $r = \infty$ to $r = a$, the electrolyte has been modeled as a spherical ohmic conductor, to obtain the commonly used formula for the access (or convergence) resistance (Hille, 1968; Andersen, 1983b; Jordan, 1987). The ohmic model does not include ion density gradients nor nonzero net charge density, both of which affect ion flux and are significant when all the current is carried by a single ion species. As a consequence, we show below that the standard formula can

lead to a 10-fold or more overestimate of the access resistance.

A formula for the limiting ion flux has been obtained by calculating the flux that would imply zero permeant ion density at the capture radius, according to simple diffusion (e.g., Andersen, 1983b). This result is valid for diffusion of neutral particles, but ignores the effect of electric potential gradients on the (non-neutral) ion flux, that are included in the Nernst-Planck and Poisson formulation, and can be important.

Läuger (1976) presented a model of ions moving radially inward toward the mouth of a channel, based on the Nernst-Planck equations (which includes ion density gradients and electric potential gradients), and solved the nonlinear problem with the a priori simplifying assumption that the net charge density is zero everywhere (rather than using the Poisson equation to relate charge density to potential). For the case of a channel with permeability large compared to the convergence permeability of the surrounding electrolyte (diffusion-limited channel) he found a limiting current in a 1–1 electrolyte that was double that predicted by simple diffusion. Assuming zero electric field at $r = a$, we find the limiting current can be any value between these limits, depending on the ratio a/λ; for nonzero field at $r = a$ it can be outside these limits.

Levitt (1985) solved the nonlinear Nernst-Planck and Poisson equations for an electrolyte-channel-electrolyte system, introducing an approximation that takes advantage of the smallness of the lipid/aqueous dielectric permittivity ratio to reduce the spatial variation to a dependence on a one-dimensional axial distance variable. The equations were integrated numerically by a Runge-Kutta method, to a finite distance into the electrolyte, where the electrolyte was assumed to be well stirred. Levitt and Decker (1988) consider a diffusion-limited channel for an experimental situation with low permeant ion density, in which the effect of ion flux on potential is negligible. They calculate the potential for zero flux. It consists of a constant field inside the channel, a Debye-Hückel potential in the bulk of the electrolyte and a third analytic expression that approximates the potential in a small transitional region between the two. Then, using this potential, the permeant ion flux is calculated from the Nernst-Planck flux equation.

In our model, we consider permeant ions converging radially toward the mouth of a conducting channel. Although the motivation is to understand its effect on ion channels, the focus in this paper is on the current-voltage-ion density relationships of the electrolyte itself. The electrolyte is assumed to extend from $r = \infty$ to a hemisphere centered on the center of the channel mouth, of radius a, equal to the mouth radius. The Nernst-Planck equations and Poisson's equation with only radial dependence are assumed to apply in this region. The assumption of radial symmetry is good for $r \gg a$ and approximately true for $r = a$, but is not valid for the region $0 \leq r < a$ in

which the field lines make a transition from predominantly radial for $r > a$ to predominantly axial inside the channel. There also might be further deviations from radial symmetry caused by fixed charges on the membrane surface or from asymmetries of the geometry of the channel mouth. By eliminating the ion densities from the equations, an integrodifferential equation for the electric potential is obtained. A simple analytic expression is obtained for the potential by linearizing the equation. It is valid when the potential drop across the electrolyte is small (compared to $kT/e = 25$ mV). When the potential is not small, the nonlinear integrodifferential equation is converted to an integral equation that is solved numerically using an iterative method and a shooting method. The linear solution is the generalization of the Debye-Hückel (1923) theory to the case of nonzero radial ion flux with a flux sink at $r = a$; the nonlinear solution is the corresponding generalization of Guggenheim's (1959) solution, or, alternatively, it is the generalization of Läuger's (1976) results to allow deviations from charge neutrality. Some of the present results have been reported (Peskoff and Bers, 1987).

MATHEMATICAL FORMULATION

Nernst-Planck Equations

The flux density of the ith ion, J_i (ions $cm^{-2} s^{-1}$), is related to the ion density, n_i (ions/cm^3), and the nondimensional electric potential, $\phi(e/kT \times$ potential in V), by the Nernst-Planck equation,

$$J_i = -D_i \left(\frac{dn_i}{dr} + z_i n_i \frac{d\phi}{dr} \right), \qquad (1)$$

where D_i is the diffusion coefficient (cm^2/s), z_i the valence, and r (cm) the radial distance variable measured from the center of the mouth of the channel, and it is assumed that ion density and electric potential vary only in the radial direction and are independent of the angular coordinates. The equations will be derived for the case of two monovalent cation species, $z_1 = z_3 = 1$, and one monovalent anion species, $z_2 = -1$, but they can be generalized to cases with divalent ions and more than three ion species.

It is assumed that only one cation species is permeable, that is,

$$J_1 = -\frac{q}{2\pi r^2}$$

$$J_2 = J_3 = 0, \qquad (2)$$

where q is the total ion flux (ions/s) entering the channel at the mouth.

The following boundary conditions are assumed. In the bulk solution, a long distance from the mouth, at $r = \infty$, the potential is zero,

$$\phi(\infty) = 0, \qquad (3)$$

and the bulk values of the ion densities are

$$n_1(\infty) = \gamma n_\infty$$

$$n_2(\infty) = n_\infty$$

$$n_3(\infty) = (1 - \gamma)n_\infty, \tag{4}$$

where γ is the bulk value of the permeable cation to anion density ratio.

Substituting Eqs. 2 in 1 and imposing the boundary conditions of Eqs. 3 and 4, the first-order differential Eq. 1 may be solved for n_i in terms of ϕ.

$$n_1(r) = \left(\gamma n_\infty - \frac{q}{2\pi D_1} \int_r^\infty \frac{\exp[\phi(r')]}{r'^2} dr'\right) \cdot \exp[-\phi(r)]$$

$$n_2(r) = n_\infty \exp[\phi(r)]$$

$$n_3(r) = (1 - \gamma)n_\infty \exp[-\phi(r)]. \tag{5}$$

Thus n_2 and n_3 are given in terms of ϕ by their familiar equilibrium values but n_1 differs from this by an integral term multiplied by the ion flux, q. This term accounts for the deviation from charge neutrality.

Poisson's Equation

To determine $\phi(r)$ another equation is needed. Poisson's equation relates the Laplacian of ϕ to the net charge density, and in spherical coordinates with only radial dependence it is

$$\frac{1}{r} \frac{d^2}{dr^2}(r\phi) = -\frac{e^2}{\epsilon kT}(n_1 - n_2 + n_3), \tag{6}$$

where ϵ is the dielectric permittivity of water.

Substituting Eqs. 5 for n_i in terms of ϕ in Eq. 6 yields a nonlinear integrodifferential equation for determining ϕ,

$$\frac{\lambda^2}{r} \frac{d^2}{dr^2}(r\phi) = \sinh \phi(r)$$

$$+ \frac{\delta}{2} \exp[-\phi(r)] \int_r^\infty \frac{\exp[\phi(r')]}{r'^2} dr', \tag{7}$$

where

$$\lambda = (\epsilon kT/2n_\infty e^2)^{1/2} \tag{8}$$

is the Debye length, and

$$\delta = q/2\pi D_1 n_\infty \tag{9}$$

is a quantity proportional to the ion flux, with dimensions of length. To obtain a physical interpretation of the distance δ, consider the simple diffusion problem of a flux q of uncharged particles (i.e., $z_i = 0$, $\gamma = 1$ in Eq. 1) converging radially toward $r = 0$. The particle density $n_1(r)$ in this case is $n_\infty(1 - \delta/r)$ and thus δ is the radial distance at which the predicted particle density would become zero. Because density cannot physically become negative, in simple diffusion δ must be less than the smallest dimension

for which the diffusion equation applies (e.g., $\delta < a$). Thus $\delta = a$ corresponds to the upper limit of particle flux for a channel of radius a. That is, there is flux (or current) saturation at $q = 2\pi a D_1 n_\infty$ (or $2\pi a D_1 \gamma n_\infty$ for $\gamma \neq 1$). It will be seen below that the inclusion of the electric force term in Eq. 1 (i.e., $z_i \neq 0$) can increase the saturation current beyond the value attainable for simple diffusion of neutral particles.

Note that as a result of the cancellation of terms containing γ in Eqs. 5, Eqs. 6 and 7 are independent of γ and hence ϕ will be independent of γ.

Nondimensionalization

It is convenient at this point to nondimensionalize the equations. The nondimensional radial coordinate is defined as

$$x = r/a, \tag{10}$$

where a is the radius of the channel mouth. Also, we introduce the dimensionless parameters,

$$\alpha = a/\lambda$$

$$\beta = \delta/2a, \tag{11}$$

and the dimensionless density,

$$N_i = n_i/n_\infty. \tag{12}$$

Using Eqs. 10 and 11 the integrodifferential Eq. 7 becomes

$$\frac{1}{\alpha^2 x} \cdot \frac{d^2}{dx^2}(x\phi(x)) = \sinh \phi(x)$$

$$+ \beta \exp[-\phi(x)] \int_x^\infty \frac{\exp[\phi(x')]}{x'^2} dx', \tag{13}$$

and the Eqs. 5 for the ion densities become

$$N_1(x) = \left[\gamma - 2\beta \int_x^\infty \frac{\exp[\phi(x')]}{x'^2} dx'\right] \exp[-\phi(x)]$$

$$N_2(x) = \exp[\phi(x)]$$

$$N_3(x) = (1 - \gamma) \exp[-\phi(x)]. \tag{14}$$

To solve the second order Eq. 13 for $\phi(x)$, one more boundary condition is needed in addition to Eq. 3. We will specify the gradient of the potential (i.e., the negative of the nondimensional electric field) at $x = 1$, and to be consistent with the spherical symmetry assumed in Eq. 6, we must assume that the electric field is constant in magnitude and in the radial direction on the surface of the hemisphere at $x = 1$. Thus we assume

$$\frac{d\phi}{dx}(1) = S, \tag{15}$$

where S is a constant. The electric field at $r = a$ is then $-kTS/ea$ V cm^{-1}.

The value of S will in general depend on the properties of the channel itself, i.e., its current/voltage relation, permeability, location of fixed charges, etc., and on the ion flux through and ion densities at both ends of the channel. In the present model it is assumed that the ion densities and electric potential in the electrolyte for $1 \leq x < \infty$ are governed by the Nernst-Planck and Poisson equations. The influence of the channel on the electrolyte is consequently totally specified by the electric field on the surface of the hemisphere at $x = 1$. Ion densities $N_i(x)$ and electric potential $\phi(x)$ in the electrolyte can be determined, given the electric field at $x = 1$, the ion flux in the system and the boundary values $n_i(\infty)$ and $\phi(\infty)$. However, for a channel between two electrolytes with, say, the ion flux through the system given, it would be necessary to determine the magnitude of the electric field at $x = 1$ that simultaneously satisfies the electrolyte and channel models, i.e., yields continuity of electric field at $x = 1$.

In the next section we will derive an analytic expression for ϕ in the special case when charge neutrality is assumed by setting the left-hand side of Eq. 13 equal to zero. This is the solution found previously by Läuger (1976). Then we will obtain a linearized solution valid when the ion flux and electric field at $x = 1$ are both small. After this we obtain an asymptotic expansion of ϕ valid for large values of x, $x \gg \beta$ and $x \gg 1/\alpha$ (or $r \gg \delta/2$ and $r \gg \lambda$), and find that the charge-neutrality solution is the first two terms of this expansion. Finally, we convert the integrodifferential Eq. 13 to an integral equation and solve it numerically using an iterative procedure for a given $\phi(1)$ and a shooting method to determine the correct $\phi(1)$.

APPROXIMATE SOLUTIONS

Charge Neutrality Solution

In most physiological models, it is permissible to assume charge neutrality, i.e., the net charge density is precisely zero everywhere. This is true when all distances of interest are large compared to the Debye length defined in Eq. 8. In the present case, it will be seen that charge neutrality occurs for $r \gg \lambda$, but not for $r \sim \lambda$. To see clearly the relationship of the approximate charge neutrality solution to the other solutions of Eq. 13 to be described, we will derive this approximation starting from Eq. 13. The a priori assumption of charge neutrality is equivalent to the right-hand side of Eq. 6, 7, or 13 being equal to zero, so that Eq. 13 becomes

$$0 = \sinh \phi(x) + \beta \exp [-\phi(x)] \int_x^\infty \frac{\exp [\phi(x')]}{x'^2} \, dx'. \quad (16)$$

Multiplying Eq. 16 by $\exp [\phi(x)]$, rearranging terms, and differentiating with respect to x yields the differential equation

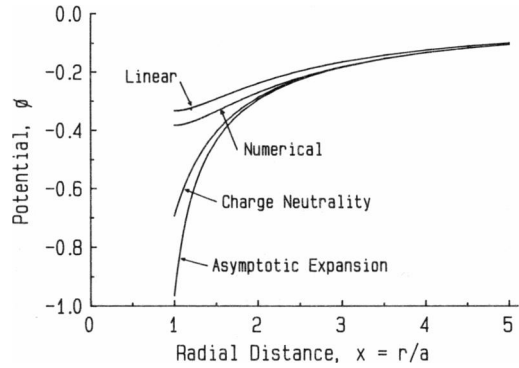$$\exp [\phi(x)] \frac{d\phi}{dx} = \frac{\beta}{x^2}. \quad (17)$$

FIGURE 1 The electric potential, ϕ, as a function of the nondimensional radial distance, $x = r/a$, for $\beta = 0.5$. The four curves are the linear approximation of Eq. 21 for $\alpha = 2$ and $S = 0$, the exact numerical solution of Eq. 39 also for $\alpha = 2$ and $S = 0$, the charge-neutrality solution of Eq. 18 and the four-term asymptotic expansion of Eqs. 25 and 31. The latter two are independent of α and S.

The solution to Eq. 17 subject to the boundary condition of Eq. 3 is

$$\phi(x) = \ln (1 - \beta/x). \quad (18)$$

This is the solution found by Läuger (1976). In Fig. 1, the curve labeled "charge neutrality" is the potential ϕ in Eq. 18, for $\beta = 0.5$ ($\delta = a$), as a function of position x, with $x \geq 1$. Substituting the potential ϕ from Eq. 18 in Eqs. 14 yields for the ion densities

$$N_1(x) = 1 - \beta/x - (1 - \gamma)/(1 - \beta/x)$$

$$N_2(x) = 1 - \beta/x$$

$$N_3(x) = (1 - \gamma)/(1 - \beta/x). \quad (19)$$

Note that the charge neutrality condition $N_1 - N_2 + N_3 = 0$ is true for Eq. 19 for all x, which was the initial assumption in Eq. 16 for this approximate solution. The permeant ion density, N_1, for $\gamma = 1$ and $\beta = 0.5$ in Eq. 19 is the curve labeled "charge neutrality" in Fig. 2.

The maximum flux (or maximum β) possible according to the charge neutrality approximation is obtained by setting $N_1(1) = 0$ in Eq. 19, yielding $\beta_m = 1 - (1 - \gamma)^{1/2}$.
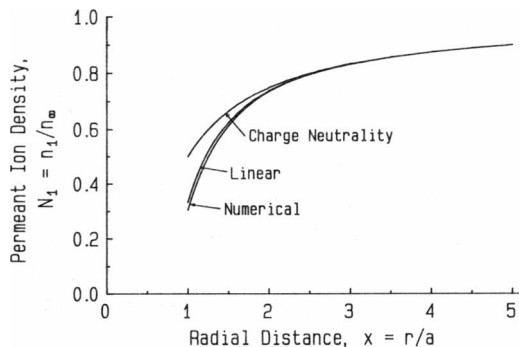

FIGURE 2 The nondimensional permeant ion density, N_1, as a function of x. The numerical solution, linearized solution and charge-neutrality solution for the same cases as in Fig. 1.

This agrees with the result of Läuger (1976) that (in the present notation) $\beta_m = 1$ for $\gamma = 1$ and $\beta_m = \gamma/2$ for $\gamma \to 0$. It should also be compared to the result for simple diffusion of neutral particles described in the paragraph following Eq. 9, which in dimensionless variables is $\beta_m = \gamma/2$ for all γ.

On the $x = 1$ hemisphere capping the mouth of the channel, according to Eq. 18, $d\phi/dx(1) = \beta/(1 - \beta)$. Consequently, it is not possible for the charge neutrality solution, Eq. 18, to satisfy the boundary condition, Eq. 15, imposed by the channel except in the special case $\beta = S/(1 + S)$. One cannot, from this derivation, determine the range of validity of Eqs. 18 and 19. It will be seen in Eqs. 25 and 31, however, that the argument of the logarithm in Eq. 18 is the leading two terms of an asymptotic expansion and Eqs. 18 and 19 are valid only if $x \gg 1/\alpha$ and $x \gg \beta$ or, in physical units, $r \gg \lambda$ and $r \gg \delta/2$. It also will be seen from the numerical solution of Eq. 13 that the potential and ion densities at the mouth of the channel, which are crucial for determining the current that flows through a channel, can differ significantly from what would be predicted by assuming that the charge neutrality solutions, Eqs. 18 and 19, are valid everywhere.

Linearized Solution

Before solving Eq. 13 numerically, we will linearize the equation and obtain a solution, valid when the potential drop across the electrolyte (from $x = \infty$ to $x = 1$) is small.

For small ϕ, letting $\sinh \phi \to \phi$ and $\exp(\pm\phi) \to 1$, Eq. 13 reduces to

$$\frac{1}{\alpha^2 x} \frac{d^2}{dx^2}(x\phi) = \phi + \frac{\beta}{x}. \tag{20}$$

The solution to Eq. 20 satisfying the boundary conditions of Eqs. 3 and 15 is

$$\phi(x) = \frac{(\beta - S)\exp[\alpha(1 - x)]}{(1 + \alpha)x} - \frac{\beta}{x}. \tag{21}$$

The curve labeled "linear" in Fig. 1 is the potential ϕ of Eq. 21 with $\beta = 0.5$, $S = 0$, and $\alpha = 2$. The right-hand side of Eq. 21 consists of two parts. One part is the potential induced by the ion flux, the terms proportional to β. This contains a term that decays as an exponential divided by x, and a less rapidly decaying $-\beta/x$ term. The potential does not become zero at any finite x but falls off as $-\beta/x$ as $x \to \infty$ to be consistent with the radially inward ion flux. The other part is induced by the electric field emanating from the channel, the term proportional to S. It is the familiar Debye-Hückel (1923) potential surrounding a spherically symmetric charge in an electrolyte. For an uncharged channel, this electric field is the continuation of the field within the channel that can be the force driving the ions through the channel; for a charged channel there is also a contribution from the field lines originating on the charge (see Levitt, 1985). For simplicity we have assumed

that at $x = 1$ this electric field is constant and directed radially, although this is obviously an approximation to the true situation. The true situation, if known, would require the solution to a much more complicated mathematical problem.

Note that Eq. 21, the linearized solution, has the same behavior for large x as Eq. 18, the charge-neutrality solution. This is seen by dropping the exponential term in Eq. 21 and by expanding the logarithm in Eq. 18 in a Taylor series so that $\ln(1 - \beta/x) \to -\beta/x$ as $\beta/x \to 0$.

For $\beta \geq 0$ and $S \geq 0$ ($\beta \leq 0$ and $S \leq 0$), corresponding to ion flux and electric field in the negative (positive) x direction, $\phi(x)$ in Eq. 21 has a maximum magnitude of $(\alpha|\beta| + |S|)/(1 + \alpha)$ at $x = 1$ and is negative (positive). For β and S of opposite signs the maximum magnitude is smaller and occurs at $x > 1$. We now consider under what conditions $\phi(x)$ is sufficiently small for the linearization of Eq. 20 to be valid. To obtain Eq. 20 from Eq. 13 two approximations were made: replacing $\exp(\pm\phi) = 1 \pm \phi + \phi^2/2! \pm \ldots$ by 1 in the second term on the right-hand side of the equations, which is valid if $|\phi| \ll 1$, and replacing $\sinh \phi = \phi + \phi^3/3! + \ldots$ by ϕ, which is valid for the less restrictive condition $\phi^2 \ll 6$. Therefore, Eq. 20 is certainly a good approximation if $|\phi| \ll 1$. However, if $\alpha|\beta|/(1 + \alpha)$ is very small but $|S|/(1 + \alpha)$ is not so small, the second term on the right-hand side of Eq. 20 has a relatively small effect on the solution in Eq. 21 and therefore it is less important that $\exp(\phi)$ is approximated well by 1 than it is that $\sinh \phi$ is approximated well by ϕ. Consequently, Eq. 21 will be valid if $|\phi| \ll 1$, or also under the less restrictive conditions $\alpha|\beta|/(1 + \alpha) \ll 1$ and $\phi^2 \ll 6$. To put this in physical terms, the linear approximation of Eq. 21 will be valid for somewhat larger magnitudes of ϕ when ϕ is dominated by the electric field at the mouth ($S \gg \alpha|\beta| = |\delta|/2\lambda$) and the ion flux is small ($\alpha|\beta|/(1 + \alpha) = |\delta|/2(\lambda + a) \ll 1$) than when the ion flux is itself large enough to cause a significant potential. Thus, the linearized solution of Eq. 20 is valid if

$$(\alpha|\beta| + |S|)/(1 + \alpha) \ll 1 \tag{22a}$$

or if

$$\alpha|\beta|/(1 + \alpha) \ll 1 \text{ and } S^2/(1 + \alpha)^2 \ll 6. \tag{22b}$$

As a numerical example, let $a = 0.2$ nm and $\lambda = 1$ nm so that $\alpha = 0.2$. Assume a channel of length ℓ with a potential difference $\Delta\phi$ across it. Also, make the approximation (Levitt, 1985) that the field on the hemisphere capping the mouth (area $2\pi a^2$) is reduced to one-half its value inside the channel (cross-sectional area πa^2). Then, from Eq. 15, $S = a\Delta\phi/2\ell$. For $a = 0.2$ nm, $\ell = 4$ nm and $\Delta\phi = 4$ (100 mV in physical units), $S = 0.1$. Calculating β from Eqs. 9 and 11, for an ion current, $qe = 10^{-12}$ amps, $D_1 = 1.3 \times 10^{-5}$ cm^2/s and a concentration (n_∞ divided by Avogadro's number) of 100 mM, $\beta = 0.03$, $\alpha\beta/(1 + \alpha) = 0.005$ and $S/(1 + \alpha) = 0.09$. In this case, according to inequalities

22b, we expect Eq. 21 to be a good approximation for the potential.

If inequalities 22b hold but inequality 22a does not, $N_i(x)$ is obtained by substituting the linear approximation for ϕ, Eq. 21, in the exact formula for $N_i(x)$, Eq. 14. If the condition 22a holds, i.e., if $|\phi| \ll 1$, a linear approximation for $N_i(x)$ can be obtained. Letting $\exp(\pm\phi) \to 1$ in Eqs. 14, the linearized ion densities are

$$N_1(x) = \gamma[1 - \phi(x)] - 2\beta/x$$

$$N_2(x) = 1 + \phi(x)$$

$$N_3(x) = (1 - \gamma)[1 - \phi(x)], \qquad (23)$$

where $\phi(x)$ is given by Eq. 21. The curves labeled "linear" in Figs. 1 and 2 are the potential, $\phi(x)$, and the density, $N_1(x)$, of Eqs. 21 and 23 for $\gamma = 1$, $\beta = 0.5$ and $\alpha = 2$.

The net charge density is en_∞ times

$$N_1 - N_2 + N_3 = -2\phi - 2\beta/x$$

$$= -2(\beta - S) \exp[\alpha(1 - x)]/[(1 + \alpha)x]. \quad (24)$$

According to Eqs. 21 and 23, each ion species density varies as $1/x$ for large x. However, according to Eq. 24, the net charge density has no $1/x$ term but decreases as $\exp(-\alpha x)/x$ with increasing x. Thus, for $x \gg 1/\alpha$, i.e., for $r \gg \lambda$, the net charge density rapidly approaches zero and charge neutrality is attained.

Note that linearization restricts $|\phi|$ but there is no corresponding restriction on N_i, which can be any value between 0 and 1.

As an example of how Eq. 23 can be used to predict the maximum current that can pass through a channel (the "electrodiffusion-limited" current), assume the capture radius is equal to the channel radius. The maximum attainable value of β is then obtained by setting $N_1(1) = 0$ in Eq. 23 with the result

$$\beta_m = \frac{\gamma(1 + \alpha + S)}{2 + \alpha(2 - \gamma)}.$$

For $\gamma = 1$, and the other values as in the above example, $\beta_m = 0.6$, corresponding to a limiting current of 2×10^{-11} amps.

If the capture radius is greater than the channel radius the above analysis is unchanged if $r = a$ is interpreted as the capture radius rather than as the channel radius, and S as the field at the capture radius. However, if the capture radius is less than the channel radius this analysis cannot be applied without modification because the radial symmetry assumption breaks down at distances less than the channel radius.

Asymptotic Expansion for Large x

It is useful to obtain an asymptotic expansion of $\phi(x)$ for large x for evaluating the portion of the integral in Eq. 13 between some large value of x and infinity. Dani (1986)

and Levitt (1985), in their computations, impose the condition that the potential is zero at some finite distance for the channel. In our model, $\phi(x)$ is zero at $x = \infty$, but using the asymptotic expansion for large x reduces the range of x over which it is necessary to integrate numerically. The asymptotic expansion is a refinement of the charge neutrality solution of Eq. 18 (the first two terms of the asymptotic expansion are the two terms in Eq. 18). Motivated by the form of Eq. 18, we transform Eq. 13 to an equation with the dependent variable

$$u(x) = \exp(\phi) \qquad (25)$$

rather than ϕ,

$$\frac{1}{\alpha^2 x}\frac{d^2}{dx^2}(xu) - \frac{1}{\alpha^2 u}\left(\frac{du}{dx}\right)^2 = \frac{u^2}{2} - \frac{1}{2} + \beta \int_x^\infty \frac{u(x')}{x'^2}dx', \quad (26)$$

and we make the further change of dependent variable to

$$v(x) = u(x) - (1 - \beta/x), \qquad (27)$$

and obtain the equation for v,

$$\frac{1}{\alpha^2 x}\frac{d^2}{dx^2}(xv) - \frac{1}{\alpha^2}\left(1 - \frac{\beta}{x} + v\right)^{-1}\left(\frac{dv}{dx} + \frac{\beta}{x^2}\right)^2$$

$$= v\left(1 - \frac{\beta}{x} + \frac{v}{2}\right) + \beta \int_x^\infty \frac{v(x')}{x'^2}dx'. \quad (28)$$

Substituting the asymptotic series

$$v(x) = a_0 + a_1 x^{-1} + a_2 x^{-2} + \cdots \qquad (29)$$

in Eq. 28 multiplied by $(1 - \beta/x + v)$ and equating terms of equal powers of x (up to x^{-5}) on the two sides of the equation to determine the coefficients, yields

$$a_0 = a_1 = a_2 = a_3 = 0$$

$$a_4 = -\beta^2/\alpha^2$$

$$a_5 = -9\beta^3/5\alpha^2 \qquad (30)$$

so that, from Eqs. 27, 29, and 30,

$$u(x) = 1 - \frac{\beta}{x} - \frac{\beta^2}{\alpha^2 x^4}\left(1 + \frac{9\beta}{5x} + \cdots\right)$$

$$= 1 - \frac{\delta}{2r} - \frac{\delta^2\lambda^2}{4r^4}\left(1 + \frac{9\delta}{10r} + \cdots\right). \qquad (31)$$

The sum of the four terms in the asymptotic expansion 31 is a good approximation to $u(x)$ if $x \gg \beta$ and $x \gg 1/\alpha$, or in physical variables, if $r \gg \delta/2$ and $r \gg \lambda$. The curve labeled "asymptotic expansion" in Fig. 1 is $\ln[u(x)]$ from Eq. 31 with $\beta = 0.5$ and $\alpha = 2$.

Substituting u from Eq. 31 in the right-hand side of Eq. 26, or v from Eqs. 29 and 30 in Eq. 28, yields an asymptotic formula for the net charge density for large x. It is $-en_\infty\beta^2/\alpha^2 x^4 + \ldots$, which indicates a slower approach to charge neutrality than the exponential approach predicted

by the linear analysis, Eq. 24, but with a coefficient that is normally very small ($\sim\beta^2$) so that this would dominate the exponential only at very large αx.

EXACT SOLUTION

Integral Equation

Eq. 13 can be written as

$$\frac{d^2}{dx^2}[x\phi(x)] = f[x, \phi(x)], \tag{32}$$

with

$$f[x, \phi(x)] = \alpha^2 x\{\sinh \phi(x) + \beta \exp[-\phi(x)]$$

$$\cdot \int_x^\infty \frac{\exp[\phi(x')]}{x'^2}\, dx'\}. \tag{33}$$

Integrating Eq. 32 once from 1 to x,

$$\frac{d}{dx}[x\phi(x)] - \frac{d\phi}{dx}(1) - \phi(1) = \int_1^x f(x', \phi(x'))\, dx', \tag{34}$$

and integrating a second time from 1 to x, Eq. 34 becomes

$$[x\phi(x) - \phi(1)] - (x - 1)\left[\frac{d\phi}{dx}(1) - \phi(1)\right]$$

$$= \int_1^x \int_1^{x'} f(x'', \phi(x''))\, dx''dx'. \tag{35}$$

Rearranging the left-hand side of Eq. 35, dividing by x, reversing the order of integration of the double integral and then performing the inner integration yields

$$\phi(x) = \phi(1) + \left(1 - \frac{1}{x}\right)\frac{d\phi}{dx}(1)$$

$$+ \int_1^x \left(1 - \frac{x'}{x}\right)f(x', \phi(x'))\, dx'. \tag{36}$$

Eq. 36 is a nonlinear integral equation which may be solved numerically to determine $\phi(x)$ for a given $\phi(1)$ and $d\phi/dx(1)$.

Another integral equation can be derived by letting $x = \infty$ in Eq. 36 and using the $\phi(\infty) = 0$ boundary condition of Eq. 3, yielding

$$\phi(1) = -\frac{d\phi}{dx}(1) - \int_1^\infty f(x', \phi(x'))\, dx' \tag{37}$$

and then substituting Eq. 37 in Eq. 36, obtaining

$$\phi(x) = -\frac{1}{x}\frac{d\phi}{dx}(1) - \left(\int_1^x \frac{x'}{x} + \int_x^\infty\right)f(x', \phi(x'))\, dx'. \tag{38}$$

Although Eq. 38 appears to be an improvement over Eq. 36, in that $\phi(1)$ has been eliminated, the iterative computation described below for Eq. 36 does not converge for Eq. 38.

Numerical Methods

The potential $\phi(x)$ has been determined numerically from Eq. 36, using an iterative technique (Hildebrand, 1965) that computes $\phi(x)$ for given values of $\phi(1)$ and $d\phi/dx(1)$, and then using a shooting method (Dahlquist and Björck, 1974) that adjusts $\phi(1)$ until $\phi(x)$ coincides for large x with the asymptotic expansion of Eqs. 25 and 31. This adjustment is equivalent to imposing the $\phi(\infty) = 0$ boundary condition so that the solution to the two-point boundary value problem with $d\phi/dx(1) = S$ (Eq. 15) and $\phi(\infty) = 0$ (Eq. 3) is obtained.

The integral from x to ∞ in Eq. 33 is replaced by the sum of the integral from x to ρ, plus the integral from ρ to ∞ in which $\phi(x')$ is replaced by its asymptotic expansion given in Eqs. 25 and 31. ρ is chosen so that Eqs. 25 and 31 are an accurate representation of $\phi(x)$ for $x \geq \rho$. Thus, for the computation, Eq. 36 is replaced by

$$\phi(x) = \phi(1) + \left(1 - \frac{1}{x}\right)S + \alpha^2 \int_1^x (x - x')\left\{\sinh \phi(x')\right.$$

$$+ \beta \exp[-\phi(x')]\left[\int_{x'}^\rho \frac{\exp[\phi(x'')]}{x''^2}\, dx''\right.$$

$$\left.+ \frac{1}{\rho} - \frac{\beta}{2\rho^2} - \frac{\beta^2}{5\alpha^2\rho^5}\left(1 + \frac{3\beta}{2\rho}\right)\right]\right\}dx'. \tag{39}$$

An initial guess $\phi^{(0)}(x)$ is made for $\phi(x)$. The precise functional form is not critical. We use a $\phi^{(0)}(x)$ which reduces to Eq. 21 when $\phi(1) = -(\alpha\beta + S)/(1 + \alpha)$, has the guessed value $\phi(1)$ and the given slope S at $x = 1$, and approaches the asymptote $-\beta/x$ exponentialy for $x \gg 1/\alpha$,

$$\phi^{(0)}(x) = \frac{(\beta - S)\exp[\alpha(1 - x)]}{(1 + \alpha)x} - \frac{\beta}{x}$$

$$+ \left[\phi(1) + \frac{\alpha\beta + S}{1 + \alpha}\right][1 - \alpha(1 - x)]\exp[\alpha(1 - x)]. \tag{40}$$

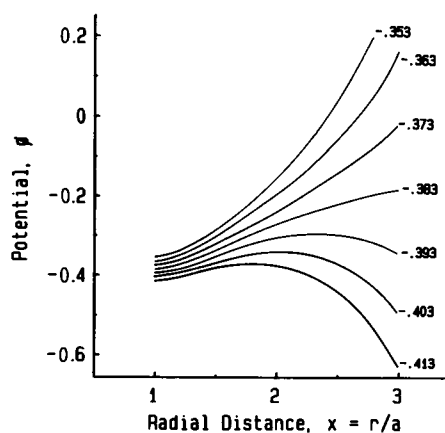FIGURE 3 Numerical computation of $\phi(x)$ from Eq. 39 for $\alpha = 2$, $\beta = 0.5$ for the correct value, $\phi(1) = -0.383$, and for six guesses of $\phi(1)$ from -0.353 to -0.413.

This $\phi^{(0)}(x)$ is substituted for $\phi(x)$ in the right-hand side of Eq. 39 and the indicated integrals performed using Simpson's rule. The resulting left-hand side, $\phi^{(1)}(x)$, is then substituted in the right-hand side of Eq. 39 yielding $\phi^{(2)}(x)$, and the process is repeated until two successive $\phi^{(k)}(x)$'s agree to within 1 part in 10^4 at $x = \rho$.

In Fig. 3 we show the result, obtained after about 20 iterations, for guesses of $\phi(1)$ from -0.353 to -0.413, for the same $\alpha = 2$, $\beta = 0.5$ case as in Figs. 1 and 2, and for $\rho = 1 + 4/\alpha = 3$ (corresponding to $r = a + 4\lambda = 3a$, a radial distance of four Debye lengths beyond $r = a$). The curve for the correct choice of $\phi(1)$, in this case $\phi(1) = -0.383$, is shown also in Fig. 1 for $1 \leq x \leq 3$ with its asymptotic tail attached for $3 \leq x \leq 5$. For $\phi(1) > -0.383$ (< -0.383) the solutions slope upward (downward) for increasing x, relative to the $\phi(1) = -0.383$ curve. The slopes of the computed $\phi(x)$ and the asymptote automatically agree at $x = \rho$, when their values agree (in this example when $\phi(1) = -0.383$). The slopes would not agree if too small a value of ρ had been selected. In the computations below, the correct $\phi(1)$ is determined by starting with an initial guess for $\phi(1)$ and then repeating the iterative process for a sequence of initial values, $\phi(1)$, adjusting successive values of $\phi(1)$ using the secant method (Dahlquist and Björck, 1974) until $\phi(\rho)$ hits the asymptotic value of $\ln [u(\rho)]$ in Eq. 31 within one part in 10^4.

We wish to compute $\phi(x)$ for selected values of α and S, and β in the range $-1 < \beta < \beta_m$. We start with small values of $|\beta|$, where the linear approximation of Eq. 21 is good, and use $\phi(1)$ from Eq. 21 for the initial guess of $\phi(1)$. As we increment the value of β, we use a quadratic extrapolation formula to obtain the initial guess $\phi(1)$ for the current value of β from the values of $\phi(1)$ already obtained for the preceeding three values of β.

The maximum value of ion flux, $\beta = \beta_m$, which occurs when the permeant ion density at the mouth, $N_1(1)$, approaches zero, is determined by adjusting β using the secant method and going through the above iteration/shooting process repeatedly until the computed value of $N_1(1)$ from Eq. 14 satisfies $|N_1(1)| < 10^{-5}$.

Numerical Results

The curves in Fig. 4, the results of the numerical solution of Eq. 39, are radial profiles of the nondimensional electric potential, ϕ. The curves are for $\beta = 0.5$, $S = 0$ (the same values as in the previous examples), and $\alpha = 0.25, 0.5, 1, 2, 4$, and ∞. The numerical integration for the upper five curves was done over the range $1 \leq x \leq \rho = 1 + 4/\alpha = 17$, 9, 5, 3, and 2, respectively. For the $\alpha = 2$ and 4 curves the asymptotic tail of Eqs. 25 and 31 was used for $3 < x \leq 5$ and $2 < x \leq 5$, respectively. The $\alpha = \infty$ curve is the change-neutrality solution of Eq. 18, because setting $\alpha = \infty$ in Eq. 13 yields Eq. 16. The curves become indistinguishable from the $\alpha = \infty$ curve beyond $x = 1 + 3/\alpha$ or $r = a + 3\lambda$.

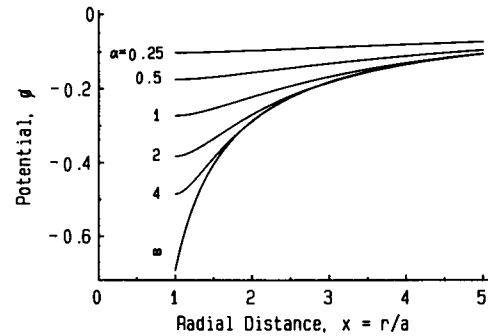Fig. 5 A shows the relationship between the nondimen-

FIGURE 4 Potential ϕ as a function of x, from the numerical solution of Eq. 39, for $\alpha = 0.25, 0.5, 1, 2$, and 4, $\beta = 0.5$ and $S = 0$. The $\alpha = \infty$ curve is the charge-neutrality solution, $\phi = \ln (1 - 0.5/x)$.

sional ion flux, β, and the potential at the mouth of the channel, $\phi(1)$, for different values of the channel-radius-to-Debye-length ratio, $\alpha = 0, 0.25, 1, 4, 16$, and ∞. Each solid curve is the nondimensional current/voltage relation across the electrolyte, from $x = 1$ to $x = \infty$, because $\phi(\infty) = 0$, for the indicated value of α. The dotted curves represent saturation flux β_m for permeable ion to anion density ratios $\gamma = 1, 0.75$, and 0.5 (top to bottom) obtained by setting $N_1(1) = 0$ in Eq. 14. If β is negative (outgoing flux) there is
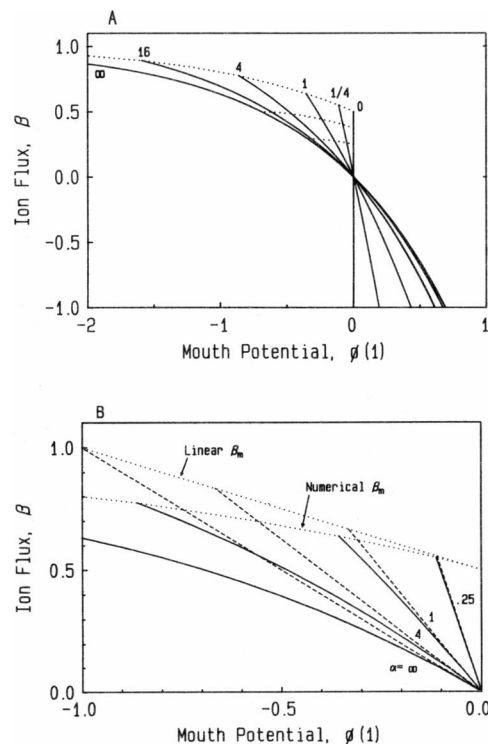

FIGURE 5 (A) The solid curves are ion flux, β, vs. potential at the mouth of the channel, $\phi(1)$, for $\alpha = 0, \frac{1}{4}, 1, 4, 16$, and ∞. The dotted curves are the loci of the points where the permeant ion density at the mouth, $N_1(1)$, is zero for (top to bottom) $\gamma = 1, 0.75$, and 0.5. These points indicate the maximum ion flux, β_m. (B) The solid cuves are the curves from A, omitting $\alpha = 16$, for positive β. The dashed lines are the linear approximation of Eq. 21. The dotted curve and line are the loci of β_m for $\gamma = 1$, exact and linear approximation, respectively.

an accumulation rather than a depletion of permeant ions, and no saturation. The four solid curves for finite α result from the numerical solution of Eq. 39. The vertical line for $\alpha = 0$ indicates zero potential, with β varying between $-\infty$ and $\gamma/2$ (see Eqs. 41 and 42). The curve for $\alpha = \infty$ is $\beta = 1 - \exp(\phi)$, obtained by setting $x = 1$ in Eq. 18.

Fig. 5 B is a magnification of Fig. 5 A for positive β, with the addition of the β vs. $\phi(1)$ relations in the linear approximation of Eq. 21 (*dashed lines*) for direct comparison. For clarity, the $\alpha = 16$ curves and the β_m curves for $\gamma = 0.75$ and $\gamma = 0.5$ have been omitted. It is seen that for all α, the linear approximation is close to the exact solution for sufficiently small β, and for small α (e.g., $\alpha = 0.25$) the linear and exact curves are almost identical from $\beta = 0$ to $\beta = \beta_m$. These results are in general agreement with Eq. 22a and b with $S = 0$, but also show how far the linear approximation deviates from the true solution over the entire range of α and β. The β_m curve for $\gamma = 0.2$ is an almost horizontal line at $\beta \approx 0.1$ (not shown) which intersects all the current/voltage curves in their linear range. Thus, if $\gamma < 0.2$ (i.e., the permeant cation concentration is <20% of the total cation concentration) the linear approximation, Eq. 21, is good for all α.

Fig. 6 shows the electric potential profiles, $\phi(x)$, for $\alpha = 1$, $\beta = 0.1$, for electric field strengths at the channel mouth in the physiological range $-0.2 < S < 0.5$. For example, $S = 0.1$, as shown above, corresponds to the field at $a = 0.2$ nm for a 100 mV potential across an uncharged channel 4 nm in length; $S = 0.36$ corresponds to the field at $r = 0.2$ nm of a single electronic charge located at $r = 0$.

Fig. 7, A and B, show the current/voltage relation of the electrolyte for $S = 0.1$ and 0.4, $\alpha = 0, 0.25, 0.5, 1, 2, 4, 8$, and ∞, and β in the range $0 \leq \beta \leq \beta_m$ for $\gamma = 1$. The curves for finite α were obtained from the numerical solution of Eq. 39. The $\alpha = \infty$ curve is from Eq. 18, which is independent of S. The $\alpha = 0$ case is a vertical line at $\phi(1) = -S$. This is the low ionic strength limit in which the ion flux does not affect the electric potential profile. This limiting case applies, for example, to the experimental conditions of Levitt and Decker (1988).

In the $\alpha = 0$ case an analytic expression can be found for β_m. Multiplying Eq. 13 by α^2 and letting $\alpha = 0$ yields
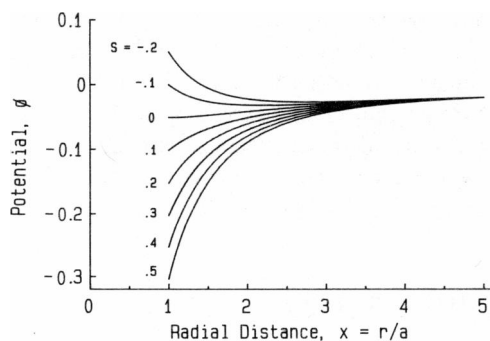

FIGURE 6   Potential ϕ as a function of x for $\alpha = 1$, $\beta = 0.1$ and nondimensional electric field at the channel mouth, $S = -0.2$ to $+0.5$.
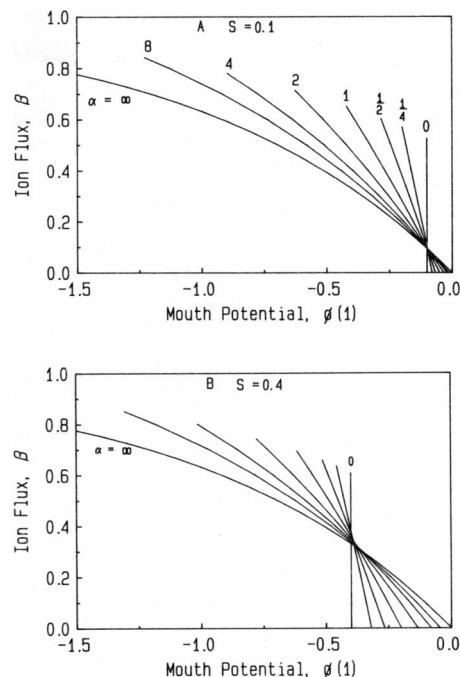

FIGURE 7   (A) Ion flux β vs. mouth potential $\phi(1)$ for a = 0, ¼, ½, 1, 2, 4, 8, and ∞ and $S = 0.1$. (B) Same as A, but $S = 0.4$.

$d^2(x\phi)/dx^2 = 0$, so that, for the boundary conditions of Eqs. 3 and 15,

$$\phi(x) = -S/x. \qquad (41)$$

Substituting this $\phi(x)$ in Eq. 14, integrating and setting $N_1(1) = 0$, yields

$$\beta_m = (\gamma S/2)/[1 - \exp(-S)], \qquad (42)$$

which gives $\beta_m = 0.5\gamma, 0.525\gamma$, and 0.607γ, for $S = 0, 0.1$, and 0.4, respectively.

The curves for different α in the $S = 0$ case of Fig. 5 A all intersect at the origin. In Fig. 7, A and B, the curves (except for $\alpha = \infty$) are shifted to the left, and the intersection becomes increasingly smeared out as S increases, occurring, for small S, over a range of points near $(-S, S)$.

Fig. 8, $A-C$, show ion density at the channel mouth, $N_1(1)$, versus ion flux, β, for $S = 0, 0.1$, and 0.4, respectively, $\alpha = 0, 0.5, 2, 8$, and ∞, and $\gamma = 1$. The $\alpha = 0$ curves are determined by substituting the potential of Eq. 41 in Eq. 14, yielding the ion density profile for $\alpha = 0$,

$$N_1(x) = \gamma \exp(S/x) - (2\beta/S)[\exp(S/x) - 1]. \qquad (43)$$

Setting $\gamma = 1$ and $x = 1$ in Eq. 43 gives the equation of the straight lines for $\alpha = 0$ in the figures. The curves for finite α are obtained by substituting the numerical solution of Eq. 39 in Eq. 14. The $\alpha = \infty$ case, obtained from Eq. 19 with $x = 1$, is the straight line $N_1(1) = 1 - \beta$, independent of S. The $S = 0$ curves intersect at $(0, 1)$; the $S = 0.1$ and 0.4 curves have a smeared intersection that for small S is
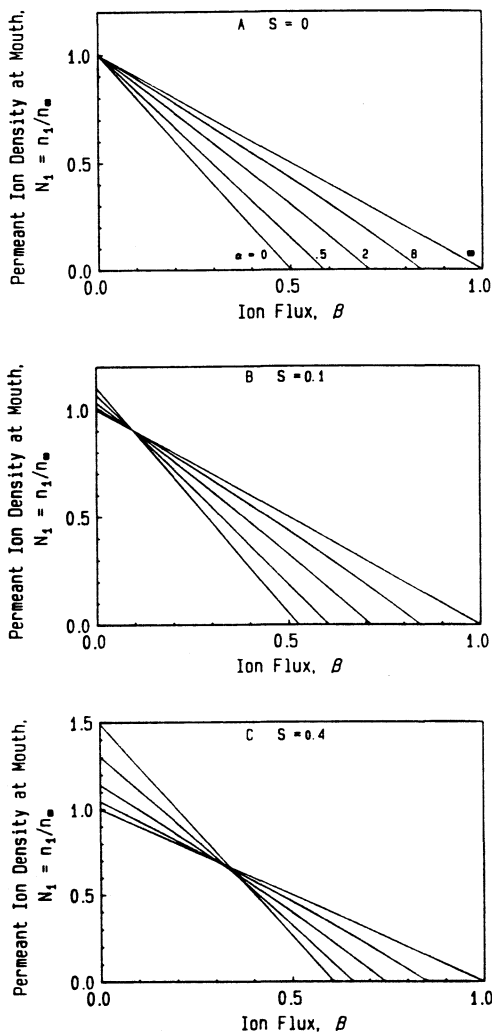
FIGURE 8 (*A*) Permeant ion density at channel mouth, $N_1(1)$, vs. ion flux, β, for $\alpha = 0, 0.5, 2, 8$, and ∞ and $S = 0$. (*B*) Same as *A*, but $S = 0.1$. (*C*) Same as *A*, but $S = 0.4$.

near $(S, 1 - S)$. A comparison of the three sets of curves in Fig. 8, *A* –*C*, shows that there is a significant increase in the permeant cation density as the inward electric field at the mouth increases in magnitude. This increase in density results from the inwardly directed force of the electric
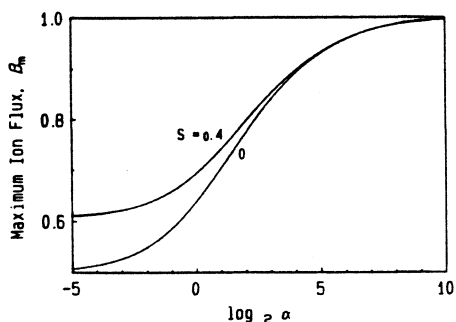

FIGURE 9 Maximum ion flux, β_m, vs. $\log_2 \alpha$ for $\gamma = 1$ and $S = 0$ and 0.4. These curves are the β values at the tops of the solid curves in Fig. 5 *A* and 7 *B* with $\log_2 \alpha$ as the independent variable rather than $\phi(1)$.

field. It becomes less pronounced as α increases because the Debye screening of the electric field becomes more pronounced as α increases.

Fig. 9 shows the maximum flux, β_m for $\gamma = 1$ as a function of the channel radius to Debye length ratio, α, in the range $\frac{1}{32} \leq \alpha \leq 1,024$. These are the same points as in the loci of the tops of the curves in Figs. 5 *A* and 7 *B*, with α as independent variable rather than $\phi(1)$. For large α, β_m becomes independent of S. However, Fig. 9 extends to large values of α that are unlikely to be physiologically relevant.

ACCESS RESISTANCE

Access resistance can be defined as the voltage drop across the electrolyte resulting from the flow of ions, divided by the ion current. If the electrolyte is modeled as an ohmic conductor, the ion current is simply proportional to the electric field. This is equivalent to ignoring the density gradient term in Eq. 1, so that from Eqs. 1 and 2,

$$J_1 = -D_1 n_\infty d\phi/dr = -q/2\pi r^2. \tag{44}$$

Integrating from a to ∞ and using Eq. 3,

$$\phi(r) = -q/2\pi r D_1 n_\infty. \tag{45}$$

The access resistance is then

$$R_{acc} = (kT/e)[\phi(\infty) - \phi(a)]/qe = kT/2\pi e^2 a D_1 n_\alpha. \tag{46}$$

Eq. 46 is the generally used formula for access resistance (Hille, 1968; Hall, 1975).

Using Eq. 18 for ϕ instead of Eq. 45, we can obtain a formula that includes density gradients but assumes charge neutrality. Assuming that $\beta \ll 1$ and therefore $\ln (1 - \beta) \approx -\beta$, Eq. 18, yields, using Eqs. 9 and 11,

$$R_{acc} = (kT/e)\beta = kT/4\pi e^2 a D_1 n_\alpha. \tag{47}$$

This is one-half times the result in Eq. 46. The decrease results because the density gradient facilitates the flow of ions.

Using Eq. 21 for ϕ we can obtain a formula for R_{acc} that also includes the effect of nonzero net charge density. To include the possibility that $S \neq 0$ in Eq. 15, it is necessary to generalize the definition of access resistance to take into account the nonzero potential that exists across the electrolyte for zero current when there is a nonzero electric field at the mouth. In this case, access resistance can be defined as the difference between the electric potential drop across the electrolyte, $-(kT/e)\phi(1)$, for current qe, and the potential drop for zero current, divided by the current,

$$R_{acc} = \frac{kT[\phi(1) - \phi(1,q=0)]}{qe^2}$$

$$= \frac{kT}{4\pi e^2(a + \lambda)D_1 n_\alpha} = \frac{\lambda^2}{2\pi\epsilon(a + \lambda)D_1}, \tag{48}$$

where Eqs. 9 and 11 and the linearized ϕ of Eq. 21 were used to get the second equality in Eq. 48. The third equality in Eq. 48, obtained using Eq. 8, is given to illustrate clearly the dependence of R_{acc} on λ. Comparing Eqs. 48 and 47 shows that deviations from charge neutrality result in a multiplication of R_{acc} by $a/(a + \lambda)$. This is equivalent to the effect of an increase of the radius from the channel radius, a, to the channel radius plus one Debye length, $a + \lambda$. If, for example, $\lambda = 0.8$, nm and $a = 0.2$ nm, Eq. 48 yields a reduction of R_{acc} by a factor of 10 compared with Eq. 46.

ELECTRODIFFUSION-LIMITED CHANNEL

Up to this point we have considered only the relationship of ion flux, ion density, and electric potential within the confines of the electrolyte, $1 \leq x < \infty$ $(a \leq r < \infty)$. To relate the results to the experimental situation of a channel with electrolytes on both sides, we shall now consider the idealized electrodiffusion-limited channel (Läuger, 1976; Andersen, 1983b; Levitt and Decker, 1988) between symmetric electrolytes. In this idealization, the ion flux, by definition, is limited totally by electrodiffusion in the $1 \leq x < \infty$ electrolyte in which there is an inward ion flux. The potential drop across the channel, assumed to extend from $x = 1$ on the right to $x = -(\ell/a) - 1$ on the left, is thus the equilibrium potential

$$\Delta\phi = \phi(1) - \phi(-(\ell/a) - 1) =$$
$$\ln [N_1(-(\ell/a) - 1)/N_1(1)]. \quad (49)$$

The left electrolyte extends from $x = -(\ell/a) - 1$ to $x = -\infty$. The potential from $x = \infty$ to $x = -\infty$ is then

$$\phi(\infty) - \phi(-\infty) = [\phi(\infty) - \phi(1)] + \ln [N_1(-(\ell/a) - 1)/N(1)]$$
$$+ [\phi(-(\ell/a - 1) - \phi(-\infty)], \quad (50)$$

which is the sum of potential drops across the right electrolyte, the channel, and the left electrolyte. The potential in Eq. 50 is shown in Fig. 10 versus ion flux for $\gamma = 1, S = 0$, and $\alpha = 0, 0.5, 2, 8,$ and ∞.
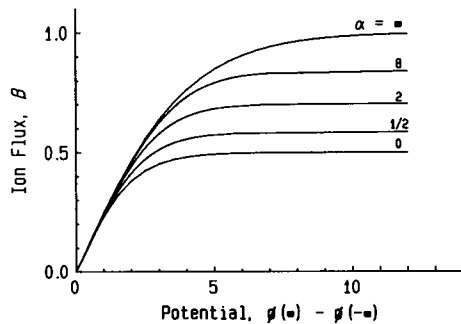
FIGURE 10 Ion flux β vs. potential drop $\phi(\infty) - \phi(-\infty)$ across an electrodiffusion-limited channel and two symmetric electrolytes, for $\gamma = 1$, $\alpha = 0, \frac{1}{2}, 2, 8,$ and ∞, and $S = 0$. The $\alpha = 0$ curve is $\phi(\infty) - \phi(-\infty) = \log [(1 + 2\beta)/(1 - 2\beta)]$; the $\alpha = \infty$ curve is $\phi(\infty) - \phi(-\infty) = 2 \log [(1 + \beta)/(1 - \beta)]$.

The $\alpha = 0$ curve is obtained by noting that when $\alpha = S = 0$, from Eq. 41 the potential across each electrolyte is zero, and from Eq. 43 with $\gamma = 1$ and $S = 0$, $N_1(1) = 1 - 2\beta$ (flux inward), $N_1(-(\ell/a) - 1) = 1 + 2\beta$ (flux outward), and therefore from Eq. 50, $\phi(\infty) - \phi(-\infty) = \ln [1 + 2\beta)/(1 - 2\beta)]$. For the $\alpha = \infty$ curve, from Eq. 18, the potential drops across the right and left electrolytes are $\ln (1 - \beta)$ and $-\ln (1 + \beta)$, respectively, and from Eq. 19, $N_1(1) = 1 - \beta$, $N_1(-(\ell/a) - 1) = 1 + \beta$ and therefore from Eq. 50, $\phi(\infty) - \phi(-\infty) = 2 \ln [(1 + \beta)/(1 - \beta)]$. The curves for $\alpha = 0.5, 2,$ and 8 were obtained using the numerical solution of Eq. 39 for $\phi(x)$, substituting $\phi(x)$ in Eq. 14 to obtain $N_1(a)$ and $N_1(-(\ell/a) - 1)$, and using Eq. 50. The $\alpha = \infty$ curve was obtained by Läuger (1976) under the assumption of charge neutrality. The curves for different α coincide approximately in the range $0 \leq \beta \leq 0.25$ but for larger values of β the differences are large.

It is of interest to observe what fraction of the total potential drop occurs across the channel. For $\alpha = 0$, there is no potential drop across the electrolyte; all the drop occurs across the channel. For $\alpha = \infty$, half the drop is across the channel and half is across the two electrolytes. For all α, according to Fig. 10, the potential across the electrolyte-channel-electrolyte system approaches infinity as the ion flux approaches the limiting value β_m. However, Fig. 5 A shows that, except for $\alpha = \infty$, the potential across the electrolyte is finite, and that the maximum potential becomes smaller and smaller as α decreases. For example, if $\alpha = 0.25$ it is limited to $\phi \approx 0.1$ (2.5 mV). Consequently, as $\beta \to \beta_m$, except for $\alpha = \infty$, the voltage drop across the system appears mostly across the channel, and results mainly from ion depletion $(N_1(1) \to 0)$ rather than from the voltage drop across the access resistance.

The current/voltage curves in Fig. 10 are for the case $S = 0$, in which there is no electric field at the channel mouth, an assumption made, for example, by Dani (1986). Levitt (1985) introduced an approximation in which the field is constant inside a channel of length ℓ, and in the region $0 \leq r \leq a$ is $a^2/(a^2 + r^2)$ times its value inside the channel. The relationship between the potential $\Delta\phi$ across the channel and the field S at $r = a$ and $r = -\ell - a$ is then $S = a\Delta\phi/(2\ell + \pi a)$. In the special case of $\alpha = 0$, it is a simple matter to see how this more realistic assumption affects the results in Fig. 10. From Eqs. 43 and 49,

$$\Delta\phi = \left(\frac{2}{a} + \pi\right)S$$
$$= \ln \left[\frac{\gamma S \exp (-S) - 2\beta[\exp (-S) - 1]}{\gamma S \exp (S) - 2\beta[\exp (S) - 1]}\right]. \quad (51)$$

This may be solved for β in terms of S or $\Delta\phi$. Letting $L = (2\ell/a) + \pi$, the result is

$$\beta = \frac{\gamma\Delta\phi}{2L}$$
$$\cdot \frac{\exp ([1 + 1/L]\Delta\phi) - \exp (-\Delta\phi/L)}{1 - \exp (-\Delta\phi/L) + \exp (\Delta\phi) [\exp (\Delta\phi/L) - 1]}. \quad (52)$$

The current/voltage relation in Eq. 52 in plotted for $\gamma = 1$, $L = 40$ in Fig. 11. The $\alpha = S = 0$ result is also plotted for comparison. The effect of the nonzero field is a linear increase in β for large $\Delta\phi$ instead of saturation at $\beta = \beta_m = \frac{1}{2}$. According to Eq. 41 with $x = 1$, the potential drop across each electrolyte is S, so that from Eq. 50, $\phi(\infty) - \phi(-\infty) = \Delta\phi + 2S = [1 + (2/L)]\Delta\phi = 1.05\Delta\phi$. Similar results are expected for $\alpha \neq 0$ but require a numerical computation for obtaining values of β, $\phi(1)$, $N_1(1)$, $\phi(-(\ell/a) - 1)$ and $N_1(-(\ell/a) - 1)$ that are consistent with Eqs. 39, 14, and the equilibrium potential of the electrodiffusion-limited channel, Eq. 49.

SUMMARY

We have analyzed the electrodiffusion of ions in the aqueous medium as they move radially toward the mouth of a conducting channel. The analysis is based on the Nernst-Planck equations (Eq. 1) and Poisson's equation (Eq. 6). An integrodifferential equation (Eq. 7 or 13) is derived from the electric potential, ϕ.

By assuming charge neutrality, we obtain Läuger's (1976) solution for ϕ (Eq. 18), and formulas for the ion densities, N_i (Eq. 19).

For small ϕ we linearize the equation and obtain an analytic expression for ϕ (Eq. 21) and N_i (Eq. 23). These reduce to the Debye-Hückel (1923) solution when there is no ion flux ($q = 0$). When $q \neq 0$, in addition to the Debye-Hückel term, there is a term in ϕ proportional to q with a $(1/r)$ exp $(-r/\lambda)$ radial dependence that decays within a few Debye lengths, λ, and another with a $1/r$ radial dependence, that decays much more slowly as $r \to \infty$. The latter term is required at long distances to be consistent with the radial ion flux. The linearized solution agrees with the charge-neutrality solution if $r \gg \lambda$ and $r \gg q/4\pi D_1 n_\infty = \delta/2$. It predicts a net charge density that has a $(1/r)$ exp $(-r/\lambda)$ dependence and this implies a rapid approach to charge neutrality if $r \gg \lambda$.

An asymptotic expansion of ϕ is found (Eqs. 25 and 31) that is valid if $r \gg \lambda$ and $r \gg \delta/2$. Retaining only the first two terms reduces it to the charge-neutrality solution.
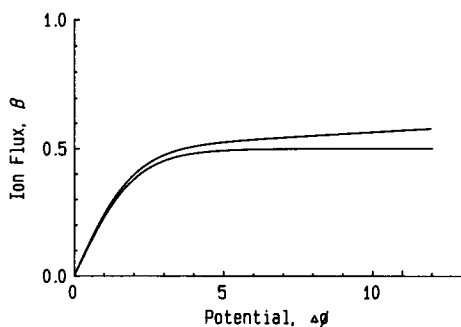
The integrodifferential equation (Eq. 13) is converted to an integral equation (Eq. 36). For arbitrary ϕ, a numerical solution is found as follows. A guess is made for ϕ at the $r = a$ boundary. An iterative method is used to find the solution for ϕ as a function of r for this guessed boundary value. The solution at $r = a + 4\lambda$ is compared with the asymptotic expansion of ϕ at $r = a + 4\lambda$. The value of ϕ at $r = a$ is adjusted, using a shooting method, until the numerical solution obtained by iteration matches the asymptotic solution at $r = a + 4\lambda$.

Families of curves are computed showing ion flux versus mouth potential and ion density at the mouth versus ion flux, for different values of a/λ and S (the nondimensional electric field at the mouth). For physiological values of a/λ ($a/\lambda \leq 0.5$) the linear flux versus potential curves agree well with the nonlinear curves, and agreement gets better as the flux decreases. The charge-neutrality solution corresponds to the numerical solution in the limit $a/\lambda \to \infty$.

The linearized solution is applied to obtain a formula for access resistance (Eq. 48) which gives a much smaller value of resistance than the previously published formula (Eq. 46; Hille, 1968).

The nonlinear solution for ion density and transelectrolyte potential as a function of ion flux, is applied to an idealized diffusion-limited channel with symmetric electrolytes. The flux versus potential curves for this electrolyte-channel-electrolyte system saturate in the $S = 0$ case (Fig. 10) at values of the flux dependent on a/λ. The saturation flux is maximum at $a/\lambda = \infty$, decreasing to half its maximum value as $a/\lambda \to 0$. For the case of constant field inside the channel diminished at $r = a$ to half its interior value ($S \neq 0$), the potential versus flux curve is obtained for $a/\lambda = 0$ (Eq. 52 and Fig. 11) which increases linearly for large potential. This result may provide an additional contribution to the explanantion of some experimental results (e.g., Andersen, 1983a; Hainsworth and Hladky, 1987) which have been attributed to ion density changes at the mouth caused by the potential drop in the Gouy-Chapman layer. Further computations, combining the present model for the electrolyte with more realistic channel models, would be necessary to evaluate this possibility.

FIGURE 11 Ion flux β vs. potential drop $\Delta\phi$ across an electrodiffusion-limited channel for $\gamma = 1$, $\alpha = 0$, and $S = a\Delta\phi/(2\ell + \pi a)$, from Eq. 52 (upper curve) and $S = 0$ (lower curve, same as in Fig. 10).

REFERENCES

Andersen, O. S. 1983a. Ion movement through gramicidin A channels: interfacial polarization effects on single-channel current measurements. Biophys. J. 41:135–146.

Andersen, O. S. 1983*b*. Ion movement through gramicidin A channels: studies on the diffusion-controlled association step. *Biophys. J.* 41:147–165.

Chapman, D. L. 1913. A contribution to the theory of electrocapillarity. *Philos. Mag. (Lond.).* 25:475–481.

Dahlquist, G., and A. Bjorck. 1974. Numerical Methods. Prentice-Hall, Inc., Englewood Cliffs, NJ. 573 pp.

Dani, J. A. 1986. Ion-channel entrances influence permeation: net charge, size, shape and binding considerations. *Biophys. J.* 49:607–618.

Debye, P., and E. Hückel. 1923. Zur theorie der elektrolyte. I. Gefrier-punktserniedrigung und verwandte erscheinungen. *Physikalische Zeitschrift.* 24:185–206.

Erdélyi, A. 1956. Asymptotic Expansions. Dover Publications, Inc., New York. 108 pp.

Gouy, G. 1910. Sur la constitution de la charge electrique a la surface d'un electrolyte. *J. Phys. Radium (Paris).* 9:457–468.

Guggenheim, E. A. 1959. The accurate numerical solution of the Poisson-Boltzmann equation. *Trans. Faraday Soc.* 55:1714–1724.

Hainsworth, A. H., and S. B. Hladky. 1987. Effects of double-layer polarization on ion transport. *Biophys. J.* 51:27–36.

Hall, J. E. 1975. Access resistance of a small circular pore. *J. Gen. Physiol* 66:531–532.

Hildebrand, F. B. 1965. Methods of Applied Mathematics. 2nd ed. Prentice-Hall, Inc., Englewood Cliffs, NJ. 362 pp.

Hille, B. 1968. Pharmacological modifications of the sodium channels of frog nerve. *J. Gen. Physiol.* 51:199–219.

Jordan, P. C. 1987. How pore mouth charge distributions alter the permeability of transmembrane ionic channels. *Biophys. J.* 51:297–311.

Läuger, P. 1976. Diffusion-limited ion flow through pores. *Biochim. Biophys. Acta.* 455:493–509.

Levitt, D. G. 1985. Strong electrolyte continuum theory solution for equilibrium profiles, diffusion limitation, and conductance in charged channels. *Biophys. J.* 48:19–31.

Levitt, D. G., and E. R. Decker. 1988. Electrostatic radius of the gramicidin channel determined from voltage dependence of H^+ ion conductance. *Biophys. J.* 53:33–38.

Peskoff, A., and D. B. Bers. 1987. Electrodiffusion of ions converging toward the mouth of a channel. *Biophys. J.* 51:395a.